Efficiency Improvement of a Class E^2 Converter for Low Power Inductive Links

Akram Bati
School of Engineering
University of Bolton
Bolton, UK

Patrick C.K. Luk
Centre for Power Engineering
Cranfield University
Cranfield, UK

Samer Aldhaher
Department of Electrical and Electronic Engineering
Imperial College
London, UK

Chan H. See
School of Engineering
University of Bolton
Bolton, UK

Raed A. Abd-Alhameed
School of Electrical Engineering and Computer Science
University of Bradford
Bradford, UK

Peter S. Excell
Wrexham Glyndwr University
Wrexham, UK

Abstract—**This work presents a model of a Class E^2 converter for wireless medium power transfer applications. The converter operates at frequency of 200 kHz and consists of an inductive link with its primary coil driven by a class E inverter and the secondary coil with voltage driven class E synchronous rectifier. A 7th order linear time invariant LTI state-space model is used to obtain the eigenvalues of the system for the four modes caused by the operation of the converter switches. A participation factor for the four modes is used to find the actual operating point dominant poles for system response. A dynamic analysis is carried out to investigate the effect of changing separation distance between the two coils based on converter performance and the changes required of some circuit parameters to achieve optimum efficiency and stability. The results show an excellent achievement in terms of efficiency (90-98%) and maintaining constant output voltage by the use of a PI controller with dynamical change of capacitors in the inverter.**

Keywords—inductive power transmission, state-space, eigenvalues, dynamic response, PI controller, DC-DC resonant converters, rectifiers, linear time invariant (LTI)

I. INTRODUCTION

Among the applications of wireless power transfer technology, DC to DC converters with inductive resonant links for high efficiency medium power applications is one of the important research activities [1-8]. These devices use class E inverters and rectifiers to form efficient high frequency DC/DC resonant converters.

In the application of class E^2 converters using inductive link for Wireless Power Transfer (WPT), researchers such as those in [1,9] used a current-driven class E rectifier. On the other hand, in order to improve the efficiency of WPT, other researchers [4-8,10] proposed a voltage-driven Class E rectifier using MOSFET instead of diode rectifier to achieve high efficiency.

However, some applications need constant output voltage for stable operation of WPT devices [10], limiting the application of the works presented in [1,4-9]. Since the distance between the transmitting circuit and the receiving circuit is not guaranteed to be fixed at a certain value, the power transferred and the output voltage change accordingly. A regulating circuit is then required to maintain a constant output voltage produced from the WPT devices. To combat this problem, the authors in [11]

suggested increasing the input voltage; however, high input voltage may lead to device breakdown due to excessive heat generated and cause lower operating efficiencies. In [12-17], authors proposed the uses of lossy, complex and bulky additional components and power consuming active devices for feedback and communications to achieve constant output voltage. Moreover, authors in [18,19] suggested a non-radiative magnetic coupling approach to deliver power more efficiently; but the effective transfer range was basically restricted to one coil diameter unless relay resonators are adopted [20]. In [21,22] an optimized circuit structure was adopted which is based on series-shunt mixed resonant circuits but these circuits produce poor efficiency especially for long separation distances, despite the complexity of the used circuits.

For the above reasons, a dynamic analysis model is required to explore all the possibilities to obtain stable high efficiency WPT devices taking into account that a control method is required in the transmitting circuit side with no cost in power consumption and keeping a good balance between constant output voltage and a high efficiency operation.

The main objectives of this work are the examination of the Linear Time Invariant (LTI) state-space model caused by the switching operation of the converter switches and the effect of MOSFET switching including the variation of the circuit parameters in terms of the dominant Eigenvalues and the complex conjugate poles of the circuit model at open loop condition. The effective Eigenvalues are calculated using participation factor and averaging through the four modes of switching in each cycle. Since the state-space model of this converter has been verified in [5], hence it is adopted in this analysis using the complex s-plane to find out the effective dominant poles that produce the circuit response under transient changes. Handling state-space models of such circuits in this manner makes the design of their controllers and regulators much easier. Most importantly the achievement of higher efficiency with dynamical change in capacitors of the inverter part of the converter as well as obtaining fairly stable and constant output voltage are currently considered here. In addition, the findings from the open loop condition will be used to build a closed loop control system with a PI controller for the proposed WPT system.
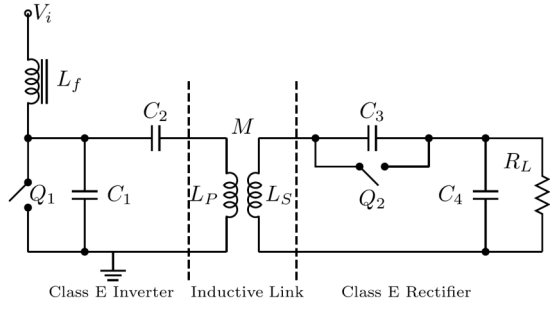
Fig. 1. Circuit of the class E² converter [5].

II. DESIGN AND METHODOLOGY

A. Mathematical Model

The circuit of Fig. 1 can be represented by the following 7th order state space equation:

$$\dot{x} = A.x + B.U$$

$$y = C.x + D.U$$

where $A = [a_{ij}]$, $B = [b_{jk}]$, $j = 1,..,7$, and $k = 1,..,7$, C is the output matrix, $U_5 = V_i$, $D = 0$, $a_{11} = \dfrac{-1}{C_1 r_{Q1}}$, $a_{15} = \dfrac{1}{C_1}$, $a_{16} = \dfrac{-1}{C}$,

$$a_{26} = \frac{1}{C_2}, \dots\dots\dots, a_{77} = \frac{\alpha r_s L_p}{M^2 (1-\alpha)}. \qquad (1)$$

For dynamic analysis, it is assumed that switching ON and OFF of the two MOSFET devices connected across C_1 and C_3 can affect the values of coefficients a_{11} and a_{33} only of the A matrix. When the switch is in ON state, these coefficients have their normal values while when they are in their OFF states these two coefficients become zero, to emulate the high OFF resistance of the device. In this case, the system transits four states representing the modes of switching in one cycle as shown in Fig. 2. The corresponding circuit transfer function can be described by the following general form:

$$\frac{Y(s)}{U(s)} = C(sI - A)^{-1} B \qquad (2)$$

where s is the complex operator of the Laplace transform of system differential equations and I is an identity matrix.

The performance of the converter circuit can be determined in terms of the input function U and the initial state of the system $x(0)$ or the initial conditions. The time domain solution can be described by the transition matrix $\varphi(t)$ and the matrices B, C are constant matrices and D is a zero matrix. $\varphi(t)$ also involves inverse Laplace transform of a matrix inversion in which $\varphi(t) = L^{-1}\{[sI - A]^{-1}\}$ where the Eigenvalues are the solution of the characteristic equation $|sI - A| = 0$.

The four modes of the switching cycle are analyzed based on the position of the dominant poles on the s-plane for which these are the nearest poles to the imaginary axis of the s-plane. A participation factor could be obtained as the ratio of each state time to the cycle period. Then at the end the effective dominant pole is determined by taking the
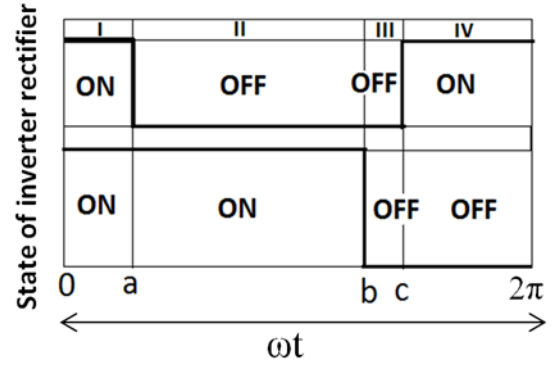
Fig. 2. The operating modes of the two MOSFETs for one switching cycle.

average of the weighted dominant poles of the four states within the switching cycle. i.e:

The dominant pole can be described by the following complex number:

$$s_d = \sigma \pm j\omega \qquad (3)$$

where s_d is the dominant pole; σ is the real part of the pole vector and should be negative for a stable system and ω is the imaginary part of the pole vector (it is also called the damped natural frequency of system response).

$\omega_n = \sqrt{\sigma^2 + \omega^2}$ is the undamped natural frequency and $\zeta = \dfrac{\sigma}{\omega_n}$ is the damping ratio of the system.

The system is stable when its dominant pole has negative real part. Let's assume f_1, f_2, f_3, and f_4 are the participation factors of the dominant poles, where

$$f_1 = \frac{a}{2\pi}, \quad f_2 = \frac{(b-a)}{2\pi}, \quad f_3 = \frac{(c-b)}{2\pi} \quad \text{and} \quad f_4 = \frac{(2\pi - c)}{2\pi}$$

Then the effective dominant pole can be found by

$$s_{dav} = \frac{f_1 s_{dI} + f_2 s_{dII} + f_3 s_{dIII} + f_4 s_{dIV}}{4} \qquad (4)$$

B. Eigenvalue Analysis and Equivalent Transfer Function

The Eigenvalues of the four switching modes shown in Fig. 2 with their dominant poles are presented in Table I. These values are obtained from Matlab based on calculation of matrix A for each switching period.

The effective eigenvalue or the dominant pole is calculated by using formula in [11] as follows: $f_1 = 0.14952$, $f_2 = 0.3504889$, $f_3 = 0.13851$, $f_4 = 0.361489$, and $s_{dav} = -1850$, where the effective transfer function will be (5).

The transfer function (5) can be reduced to:

$$TF_{av} = \frac{1850}{(s + 1850)} \qquad (6)$$

As the other poles are far away from the imaginary axis of the s-plane and have no effect on the dominant pole of the circuit. The corresponding time response of this transfer function is plotted in Fig. 3.

$$TF_{av} = \frac{1.04 \times 10^{19}}{(s + 1850)(s + 2.1 \times 10^8)(s + 2.2 \times 10^6)(s + 1.64 \times 10^4)(s^2 + s3.86 \times 10^5 + 1.1 \times 10^{12})} \qquad (5)$$
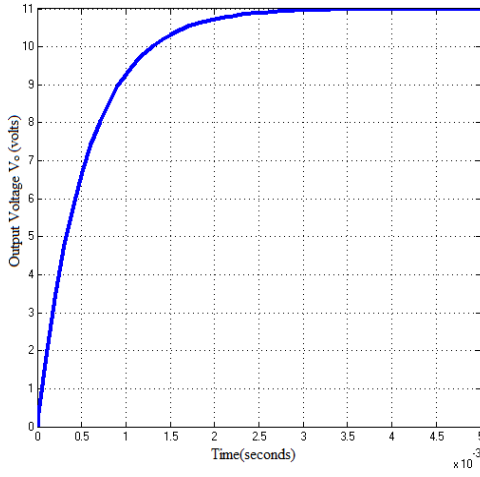
Fig. 3. Step response of the converter linearized model.

C. Linearized SIMULINK Model

In order to capture system dynamics, a linearized mathematical model is very crucial to identify system response and the purpose of the designed controller, especially if the system has time variant coefficients in the state matrix A. Linearization of this model is carried out using a built in function available in SIMULINK software based on the output and the input nodes that need to be identified.

III. SIMULATED RESULTS AND DISCUSSION

A. Effect of Parameter Variation on System Dynamic Response

Looking at the effective dominant poles, the circuit remains always stable with some amount of oscillations and this can be seen very clearly when separation distance between the primary and the secondary varies suddenly as this represents the most severe disturbance to the circuit. This response, as it is shown in Fig. 4, has been captured when separation changes from 1 mm to 8 mm.

TABLE I. THE EIGENVALUES AND THE DOMINANT POLES OF THE FOUR MODES OF SWITCHING.

Mode	Eigenvalues	Dominant pole
I	$\begin{bmatrix} -1.0057 \\ -2.1058 \\ -0.0219 \\ -0.0019 \pm j0.0103 \\ -0.0000018 \\ -0.0002 \end{bmatrix} \times 10^8$	$s_{dI} = -180$
II	$\begin{bmatrix} -1.0057 \\ -0.0005 \pm j0.0159 \\ -0.0124 \pm j0.009 \\ -0.0000018 \\ -0.0001 \end{bmatrix} \times 10^8$	$s_{dII} = -180$
III	$\begin{bmatrix} -1.2649 \pm j1.289 \\ -0.0111 \pm j1.8091 \\ -0.0015 \pm j0.1 \\ -0.009974 \end{bmatrix} \times 10^6$	$s_{dIII} = -9974$
IV	$\begin{bmatrix} -2.1058 \\ -0.0195 \\ -0.0031 \pm j0.0147 \\ -0.00000077 \pm j0.001 \\ -0.000164 \end{bmatrix} \times 10^8$	$s_{dIV} = -16400$

This figure shows the three stages of how this circuit builds up its magnetic flux first, when separation changes suddenly and finally at steady state. But practically this change takes some time so the response stays similar to that obtained in Fig. 3 or, in more detail, as in Fig. 5 where the separation distance is changing to different values repeatedly. This figure shows the responses of v_1 (voltage across capacitor 1), v_3 (voltage across capacitor 3), I_f (Inductor current), v_4 (voltage across capacitor 4), I_p (primary side current), M (the mutual inductance), and efficiency respectively.

B. Improving Converter Efficiency

To keep the converter efficiency relatively high is a real challenge to such a circuit with already chosen resonance frequency. One of the suggested methods to improve its efficiency is by changing the frequency and/or the duty ratio of the two switching devices but this entails the change of capacitor C_3 value to ensure resonance as well as changing the values of capacitor C_1 and C_2 to maximize its efficiency.

If we assume that there is no control access to the receiver side (RS) of the converter, it is better to concentrate on its transmitter side (TS). We have tried to change the values of capacitors C_1 and C_2 simultaneously with the change in separation between the TS and the RS. C_1 is increased to 70 nF and C_2 is increased to 64 nF with the change occurring in the separation. The responses look promising as a higher efficiency (90-98%) was achieved compared with what was obtained by Luk, *at el* [5]. Fig. 6 shows the efficiency achievement when the C_1 and C_2 are allowed to change simultaneously with separation change. In contrast to that very good achievement in efficiency, the change of frequency alone has a bad impact on circuit efficiency even if capacitors are changed accordingly. For example, if frequency is changed to above or below the
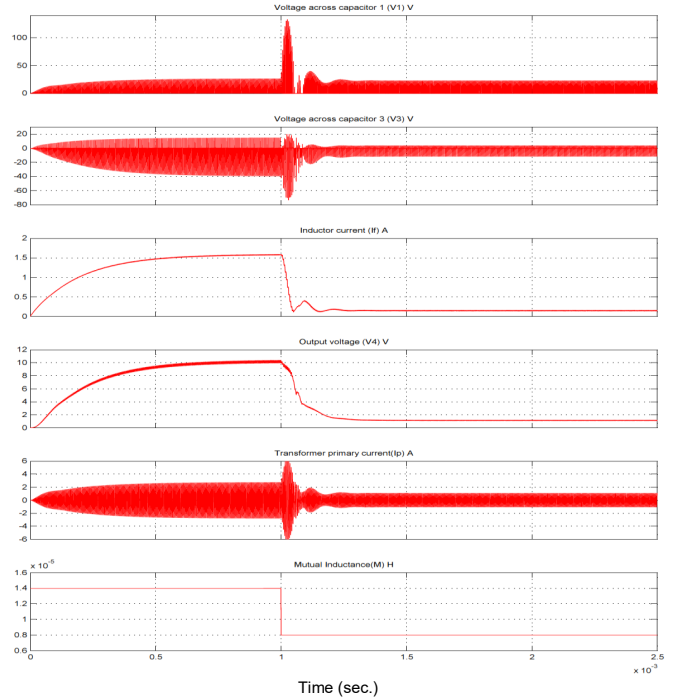
Fig. 4. Time response of the converter when separation changes from 1 mm to 8 mm, V1 (voltage across capacitor 1), V2 (voltage across capacitor 2), V3 (voltage across capacitor 3), V4 (voltage across capacitor 4), M (mutual inductance). .
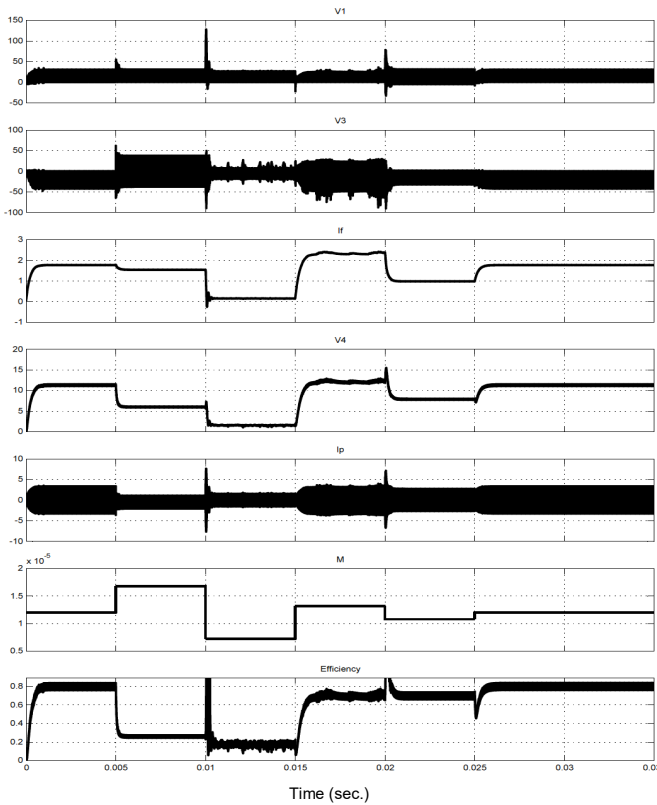
Fig.5. Time response of the converter when separation distance changes for different values.

operating frequency of 200 kHz, the result will not satisfy the required performance. For example, for 160 kHz with the required change in capacitor values the obtained efficiency is very poor (the highest reached is around 24%) as this is shown in Fig. 7. But if duty ratios of the two switches are changed simultaneously with the change of frequency as well as altering the delay angle of switch 2 without changing the values of capacitors 1 and 2, the
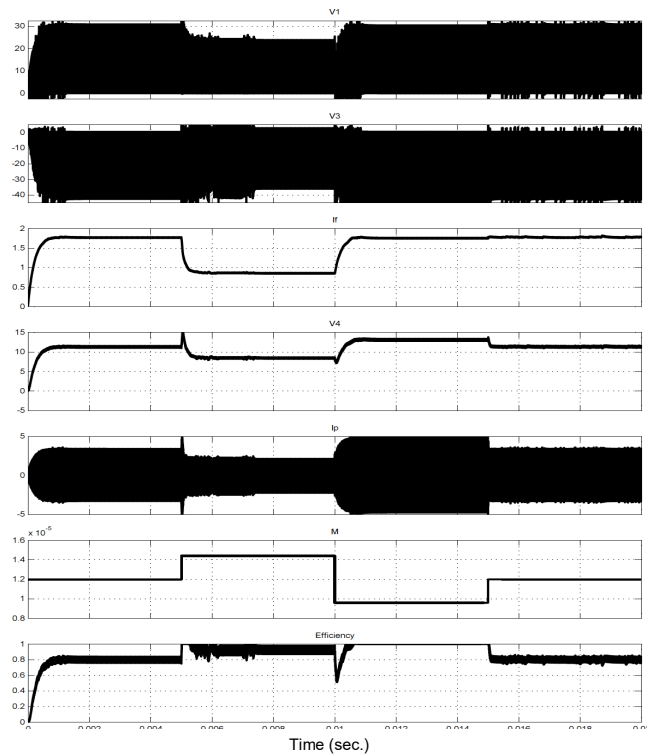
efficiency starts to improve as shown in Fig. 8, assuming fixed separation distance at 3 mm. This is confirmed by the practical tests carried out in the laboratory.

C. Maintaining Constant Voltage and High Efficiency

Fig. 9 shows the achievement of almost constant output voltage and high efficiency when separation distance changes and tuned capacitors C_1 and C_2 are used simultaneously with the change of separation between the transmitter and the receiver.

To verify the simulated results, an experiment was set up as shown in Fig. 10.

As can be seen, the class E^2 converter used in this work consists of class E zero-voltage switching (ZVS) and zero-derivative voltage switching (ZDS) inverter with an infinite DC-feed inductance, an inductive link consisting of primary and secondary coils separated by certain air gap and a voltage driven class E ZVS rectifier. The inverter and rectifier switches are named Q_1 and Q_2 respectively. The ZDS in a class E inverter means that the first derivative of the voltage across switch Q_1 is zero at the moment it is switched ON, which in turn results in zero-current switching. The switches are driven at the same switching frequency, but at different duty cycles. The converter used in the laboratory was connected to a nominal load of 10 Ω, had a coupling coefficient of 0.50 and a 200 kHz switching frequency.

The duty cycle D_1 was set to 0.50 and the one-shot timer was set to produce a 2.56 μs pulse corresponding to a duty cycle D_2 of 0.51.

The practical and simulation results which show lower efficiencies occur when separation distance between the two coils, selected capacitors values or switching frequencies are not the optimal ones. This converter achieves higher efficiencies at larger separation distances between the two coils by using properly chosen capacitors

Fig. 6. Effect of changing C_1 and C_2 on efficiency.
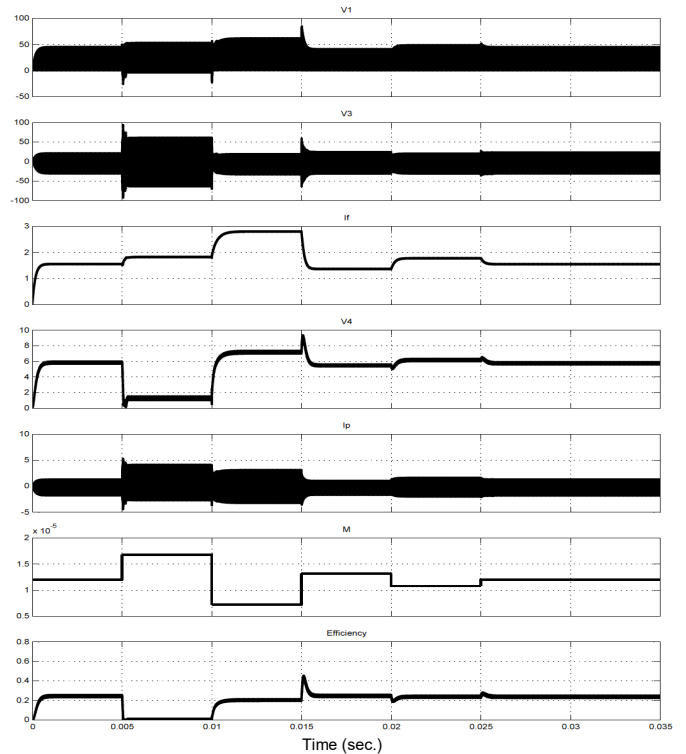
Fig. 7. Effect of frequency change on circuit efficiency.
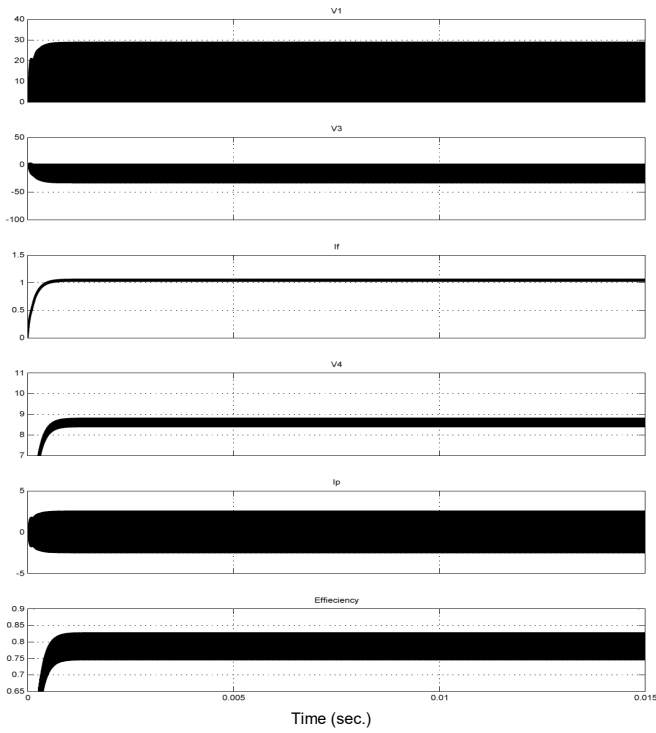
Fig. 8 Results of the converter when f = 217.243 kHz, R_L = 10Ω, D_1 = 0.444, D_2 = 0.501, delay angle of switch two = 229.982, k = 0.55.

C_1 and C_2 as shown in Fig. 9 between the times of 0.01 to 0.0145 second.

IV. EXPERIMENTAL SETUP AND VERIFICATION

The experimental setup is shown in Fig. 10. It was concluded that the circuit can achieve high levels of efficiencies if the frequency, duty ratios and delay angles of the two switching devices can be altered dynamically. This
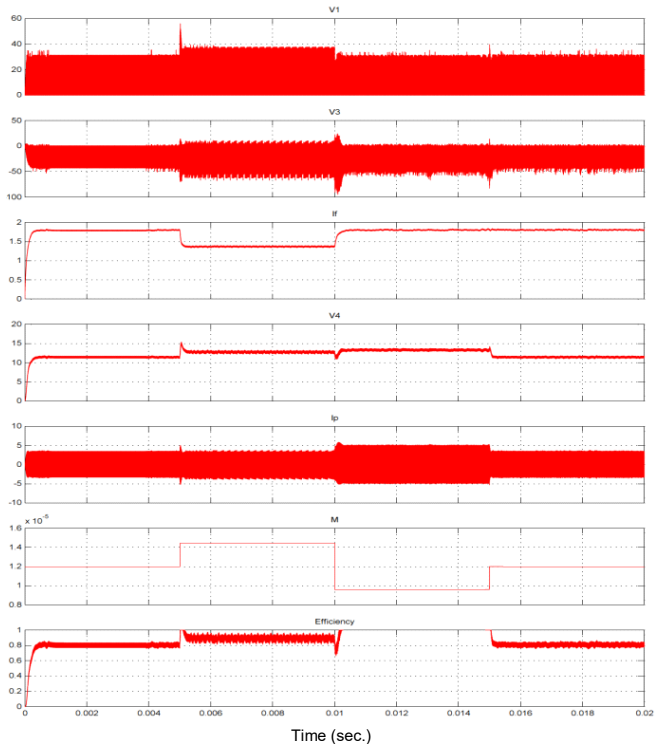
Fig. 9. Results for the converter with the aid of the PI controller.
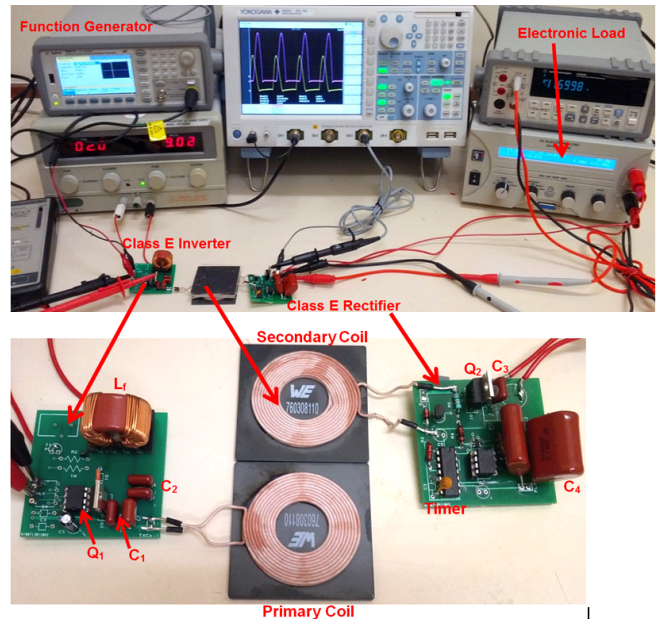
Fig. 10. Photograph of the experimental setup.

demonstrated which approach can be adopted with less cost. As can be seen in Fig. 11, the simulated and measured results are in good agreement.

V. CONCLUSION

A dynamic analysis model of the E^2 converter has been presented. The results suggest that the switching process of the MOSFET devices does not endanger stability of the circuit but changing frequency or duty ratio drifts the converter to operate at low efficiencies and cause operation instability.

Interestingly, it was found that the dynamic change of TS capacitors with the aid of a PI controller has achieved higher efficiencies and maintains constant output voltage. The feedback signal for the controller that is extracted from the available measurements in the transmitter side of the converter adds new feature for the system to be cost effective and robust and preferable for many applications where access to the receiver side of the converter is impossible or costly. The proposed work also suggested further development in the area of optimally self-tuned regulators of such type of WPT devices. This can be done by changing the capacitors in the transmitter part dynamically with the change in separation distances. The results confirmed that this produces almost constant output voltage and increased the efficiency in the proposed model.
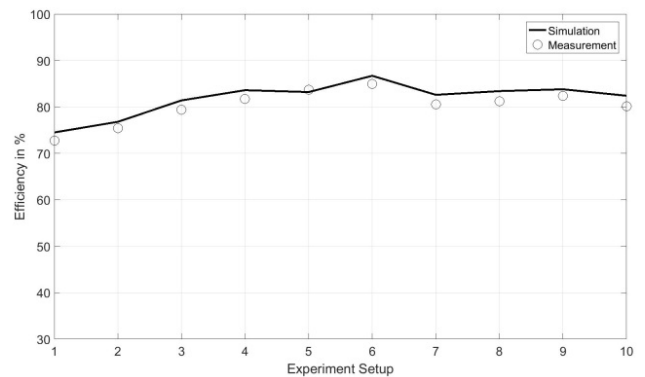
Fig.11. Simulated and measured efficiencies of the experiment setup.

REFERENCES

[1] Wireless Power Consortium. [Online] Available: http://www.wirelesspowerconsortium.com.

[2] K.V. Schuylenbergh, and R. Puers, *Inductive Powering: Basic Theory and Application to Biomedical Systems*. New York: Springer-Verlag, 2009.

[3] Qualcomm Halo. [Online] Available: http://www.qualcommhalo.com/

[4] H. Wu, G. Covic, J. Boys, and D. Robertson, "A series-tuned inductive power-transfer pickup with a controllable AC-voltage output," *IEEE Trans. Power Electron.*, vol. 26, no. 1, pp. 98–109, Jan. 2011.

[5] P.C.K. Luk, S. Aldhaher, W. Fei, and J. Whidborne, "State-space modelling of class E^2 converter for inductive links," *IEEE Trans. Power Electron.*, vol.30, no. 6, pp. 3242–3251, June 2015.

[6] S. Aldhaher, P.C.K. Luk, and J. Whidborne, "Tuning class E inverters applied in inductive links using saturable reactors," *IEEE Trans. Power Electron.*, vol. 29, no. 6, pp. 2969–2978, June 2014.

[7] S. Aldhaher, P.C.K. Luk, K. Drissi, and J. Whidborne, "High-input-voltage high-frequency class E rectifiers for resonant inductive links," *IEEE Trans. Power Electron.*, vol. 30, no. 3, pp. 1328–1335, March 2015.

[8] R.J. Calder, S.H. Lee, and R.D. Lorenz, "Efficient, MHz frequency resonant converter for sub-meter (30 cm) distance wireless power transfer," in *Proc. IEEE Energy Convers. Cong. Expo.*, 15-19 Sept. 2013, Denver, CO, USA, pp. 1917–1924.

[9] M. Pinucla, D.C. Yates, S. Lucyszyn, and P.D. Mitcheson, "Maximizing DC-to-load efficiency for inductive power transfer," *IEEE Trans. Power Electron.*, vol. 28, no. 5, pp. 2437–2447, May 2013.

[10] L. Chen, S. Liu, Y.C. Zhou, and T.J. Cui, "An optimizable circuit structure for high efficiency wireless power transfer," *IEEE Trans. Power Electron.*, vol. 60, no. 1, pp. 339–349, Jan. 2013.

[11] E. M. Thomas, J.D. Heebl, C. Pfeiffer, and A. Grbic, "A power link study wireless non-radiative power transfer system using resonant shielded loops," *IEEE Trans. Circuits and Syst. I: Regular Papers*, vol. 59, no. 9, pp. 2125–2136, Sept. 2012.

[12] S. Birca-Galateanu, and J.-L. Cocquerelle, "Class E half-wave low dv/dt rectifier operating in a range of frequencies around resonance," *IEEE Trans. Circuits and Systems I: Fundam. Theory and App.*, vol. 42, no. 2, pp. 83–94, Feb. 1995.

[13] T. Nagashima, K. Inoue, X. Wei, E. Alarcon, and H. Sekiya, "Inductively coupled wireless power transfer with class e2 dc-dc converter," in *Proc. Europ. Conf. Circuit Theory and Design (ECCTD)*, 8-12 Sept. 2013, Dresden, Germany, pp.1–4.

[14] G. Wang, W. Liu, M. Sivaprakasam, and G.A. Kendir, "Design and analysis of an adaptive transcutaneous power telemetry for biomedical implants," *IEEE Trans. Circuits Syst. I, Regular Papers*, vol. 52, no. 10, pp. 2109–2117, Oct. 2005.

[15] Q. Chen, S.C. Wong, C.K. Tse, and X. Ruan, "Analysis, design, and control of a Transcutaneous power regulator for artificial hearts," *IEEE Trans. Biomed. Circuits Syst.*, vol. 3, no. 1, pp. 23–31, Feb. 2009.

[16] P. Si., A.P. Hu, S. Malpas, and D. Budgett, "A frequency control method for regulating wireless power to implantable devices," *IEEE Trans. Biomed. Circuits Syst.*, vol. 2, no. 1, pp.22–29, March 2008.

[17] A. Moradewicz, and M. Kazmierkowski, "Contactless energy transfer system with FPGA-controlled resonant converter," *IEEE Trans. Ind. Electron.*, vol. 57, no. 9, pp. 3181–3190, Sept. 2010.

[18] Z.N. Low, R.A. Chinga, R. Tseng, and J. Lin, "Design and test of a high-power high-efficiency loosely coupled planar wireless power transfer system," *IEEE Trans. Ind. Electron.*, vol. 56, no. 5, pp. 1801–1812, May 2009.

[19] J.J. Casanova, Z.N. Low, and J. Lin, "A loosely coupled planar wireless power system for multiple receivers," *IEEE Trans. Ind. Electron.*, vol. 56, no. 8, pp. 3060–3068, Aug. 2009.

[20] Y.-H. Kim, S.-Y. Kang, M.-L. Lee, B.-G. Yu, and T. Zyung, "Optimization of wireless power transmission through resonant coupling," in *Proc. Compatibility and Power Electronics*, 20-22 May 2009, Badajoz, Spain, pp. 426–431.

[21] R.P. Severns, "Topologies for three- element resonant converters," *IEEE Trans. Power Electron.*, vol. 7, no. 1, pp. 89–98, Jan. 1992.

[22] L. Chen, S. Liu, Y.C. Zhou, and T.J. Cui, "An optimizable circuit structure for high-efficiency wireless power transfer," *IEEE Trans. Ind. Electron.*, vol. 60, no. 1, pp. 339–349, Jan. 2013.